

Data-Driven Affinely Adjustable Robust Volt/VAr Control

Naihao Shi, *Graduate Student Member, IEEE*, Rui Cheng, *Graduate Student Member, IEEE*, Liming Liu, *Graduate Student Member, IEEE*, Zhaoyu Wang, *Senior Member, IEEE*, Qianzhi Zhang, *Member, IEEE*, and Matthew J. Reno, *Senior Member, IEEE*

Abstract—Recent years have seen the increasing proliferation of distributed energy resources with intermittent power outputs, posing new challenges to the voltage management in distribution networks. To this end, this paper proposes a data-driven affinely adjustable robust Volt/VAr control (AARVVC) scheme, which modulates the smart inverter’s reactive power in an affine function of its active power, based on the voltage sensitivities with respect to real/reactive power injections. To achieve a fast and accurate estimation of voltage sensitivities, we propose a data-driven method based on deep neural network (DNN), together with a rule-based bus-selection process using the bidirectional search method. Our method only uses the operating statuses of selected buses as inputs to DNN, thus significantly improving the training efficiency and reducing information redundancy. Finally, a distributed consensus-based solution, based on the alternating direction method of multipliers (ADMM), for the AARVVC is applied to decide the inverter’s reactive power adjustment rule with respect to its active power. Only limited information exchange is required between each local agent and the central agent to obtain the slope of the reactive power adjustment rule, and there is no need for the central agent to solve any (sub)optimization problems. Numerical results on the modified IEEE-123 bus system validate the effectiveness and superiority of the proposed data-driven AARVVC method.

Index Terms—Volt/VAr control, voltage sensitivities, bidirectional search method, data-driven method.

I. INTRODUCTION

VOLT/VAr control (VVC) has always been a critical issue for power system operations. According to the standard by American National Standards Institute [1], the voltage level should be maintained within a secure range, otherwise the performance of electrical equipment might be affected. Along with the growing trend of distributed energy resources (DERs), the ability of voltage support for distribution networks also needs further improvements. According to the IEEE standard 1547-2018, proactive voltage regulations are mandatory rather than optional for power systems [2]. But considering the long reaction time and high operation cost, the legacy voltage regulation devices cannot provide dynamic voltage sup-

This material is based upon work supported by the U.S. Department of Energy’s Office of Energy Efficiency and Renewable Energy (EERE) under the Solar Energy Technologies Office Award Number 38426, and by the National Science Foundation under ECCS 1929975 and 2042314.

Naihao Shi, Rui Cheng, Liming Liu, Zhaoyu Wang and Qianzhi Zhang are with the Department of Electrical and Computer Engineering, Iowa State University, Ames, IA 50011 USA (e-mail: snh0812@iastate.edu; ruicheng@iastate.edu; limingl@iastate.edu; wzy@iastate.edu; qianzhi@iastate.edu).

Matthew J. Reno is with the Sandia National Laboratories, Albuquerque, NM 87123 USA (e-mail: mjreno@sandia.gov).

port in shorter time periods against the fluctuating voltage issues. Compared with switch-based legacy voltage regulation devices, power electronics-based smart inverters have a much shorter response time and better controllability [3]. They can both absorb or inject reactive power to eliminate the rapid voltage fluctuations across power systems. Authors in [4] claim that the high penetration of DERs may bring more difficulties in coordinating different voltage regulation devices.

In order to coordinate both the switch-based discrete devices and responsive smart inverters for voltage regulation, VVC problems in distribution networks are often formulated as optimal power flow (OPF) problems to maintain the system voltage level within a pre-defined range while accomplishing different objectives, e.g., minimizing system loss [5], reducing system cost [6] or minimizing system voltage deviations [7]. Taking full advantage of measurements, communications and control capabilities, different VVC strategies are proposed. In [8], a centralized VVC framework is proposed for day-ahead scheduling of different voltage regulation devices. To address voltage issues in different timescales caused by the stochastic and intermittent nature of DER, a robust two-stage VVC strategy is proposed in [9] to coordinate the discrete and continuous voltage regulation devices and find a robust optimal solution, which can cope with any possible realization within the uncertain DER output. However, the VVC problems in [8], [9] are solved in a centralized manner, leading to high communication costs and computational burdens. As discussed in [10], the advantages of distributed algorithms over centralized approaches in power systems include: (1) Limited information sharing, which can improve cybersecurity and protect data privacy; (2) Robustness with respect to the failure of individual agents; (3) The ability to perform parallel computations and better scalability. Distributed VVC strategies, based on the Alternating Direction Method of Multipliers (ADMM) [11] or projected Newton method, are applied to coordinate photovoltaic inverters [12], [13], and wind turbines [14], relying on the communication between neighboring buses/zones or the communication between the central agent and local agents.

In the centralized and distributed VVC strategies, the reactive power outputs of DERs highly rely on communication and coordination across distribution systems, lacking the self-regulation ability of local DERs to some extent. In order to enhance the self-regulation ability of local DERs, some local voltage control strategies are proposed to combine with the centralized and distributed VVC strategies. For instance, local voltage controls are combined with centralized/distributed

VVC strategies in [15]–[17]. The local voltage control always adjusts the reactive power outputs of DERs as a function of voltage magnitude following a given ‘Volt-Q’ piecewise linear characteristic. The characteristics and performance of droop control are tested in [18], [19]. However, according to [20], [21], the droop control may lead to some stability or feasibility issues under certain circumstances. Adaptive droop control methods are introduced in [22], [23], where the slopes and intercepts are varying in real-time to improve the stability and feasibility performance. According to IEEE 1547-2018 standard [2], it calls for supplemental capabilities – the ‘P-Q’ rule, other than the ‘Volt-Q’ rule, needed to adequately integrate DERs when the aggregated DER penetration is higher or the overall DER power output is subject to frequent large variations. For the ‘P-Q’ rule, the smart inverter’s reactive power adjustment is based on its local real-time active power rather than its voltage magnitude. More specifically, the smart inverter’s reactive power is adjusted as a function of its active power following a given/pre-defined ‘P-Q’ characteristic. In [24], the reactive power outputs of DERs are adjusted based on a quadratic relationship with the active power outputs. Researchers in [25] introduce a dynamic VVC strategy with several states, where the ‘Volt-Q’ rule and the ‘P-Q’ rule are applied to different operating statuses, respectively.

How to determine a ‘P-Q’ rule is the key to achieving good voltage regulation performances. By projecting the complex power flow relationship into linear space, the voltage deviations caused by the power injection fluctuations can be approximated rapidly [26] using voltage sensitivities. Taking advantage of voltage sensitivity analysis, different ‘P-Q’ control rules for voltage regulation are investigated. For example, in [27], an affine ‘P-Q’ rule is introduced against the voltage deviations caused by PV uncertainties, where the reactive power adjustment ratio is obtained by solving an optimization problem with voltage sensitivities as parameters. Besides, the affine ‘P-Q’ rule is further refined by incorporating voltage and inverter limit constraints in [28], resulting in fewer voltage violations and reactive power usages. But the ‘P-Q’ rules in [27], [28] are determined in a system-wise centralized manner. In [29], a network partition method is applied to divide the system into several zones, where the ‘P-Q’ rule for each zone is separately determined. That is, the ‘P-Q’ rule is determined in a zone-wise centralized manner without considering the interactions among zones. Both the system-wise and zone-wise centralized manner require a large amount of information exchanging and computational burdens. Moreover, as mentioned before, voltage sensitivities are the key parameters for performing ‘P-Q’ rules. In [27], the voltage sensitivities are calculated by inverting the Jacobian matrix, requiring a large amount of computation and system topology information. Authors in [28] utilize the surface fitting technique [30], a non-linear regression method, to estimate voltage sensitivities, where each bus voltage sensitivity is approximately calculated based on the mapping from its local power injections to its local voltage. However, this technique does not consider the influences from other buses on the local bus voltage sensitivity. The sensitivity analysis in [29] relies on the perturb and observe method, which means to repeatedly inject a small

amount of power at one node and calculate the impact on bus voltages. The perturb and observe method requires repeatedly solving the power flow.

To this end, a data-driven method is proposed for fast estimation of voltage sensitivities without requiring system topology information. Compared with conventional methods, e.g., inverting Jacobian matrices or the perturb and observe method, the proposed method is much faster. Based on the estimated voltage sensitivities, an affinely adjustable robust Volt/VAr control (AARVVC) scheme is further proposed to mitigate voltage issues against the PV uncertainty. In the first stage, the switch-based discrete devices and the base reactive power set points for PV inverters are determined with the goal of minimizing the total system power losses. In the second stage, the reactive power outputs of PV inverters are further adjusted, following a data-driven affine ‘P-Q’ control rule, to reduce possible voltage fluctuations, which is decided in a hierarchical distributed manner. The main contributions of this work are listed as follows:

- A data-driven method, based on the deep neural network (DNN), is proposed to predict voltage sensitivities. Given the voltage magnitudes and power injections of pre-selected buses as inputs, the well-trained DNNs output the corresponding voltage sensitivity parameters, which are of great importance for determining the affine ‘P-Q’ rule. It greatly improves the speed of calculating voltage sensitivities while maintaining high prediction accuracy.
- To improve the training efficiency and reduce redundant information, a feature-selection process, based on the rule-based bus selection with a Bidirectional Search (BDS) process [31], is proposed. The operating statuses of each bus, including the bus active and reactive power injections and voltages, are regarded as one feature. Then the bus-selection problem can be converted into a feature-selection problem. By applying the rule-based bus selection process, the operating statuses of a selected subset of buses, instead of the whole system, are sufficient for the fast and accurate voltage sensitivity estimation.
- The slope of the affine ‘P-Q’ rule is obtained using the consensus-based ADMM algorithm. Taking advantage of the hierarchical distributed solution structure, the optimization problem is divided into subproblems and solved by each local agent while only simple averaging calculation is processed at the center agent. It leads to lower computational burdens for the center. Additionally, relying on the communication between the central agent and local buses, the distributed consensus-based AARVVC requires less information than the system-wise and zone-wise centralized manners, which protects local information privacy.

The rest of the paper is organized as follows. Section II provides an overview of the proposed two-stage VVC strategy. The first-stage VVC strategy is formulated in Section III. Section IV presents the second-stage VVC strategy, including the data-driven voltage sensitivity estimation and the distributed consensus-based AARVVC. Numerical results on the

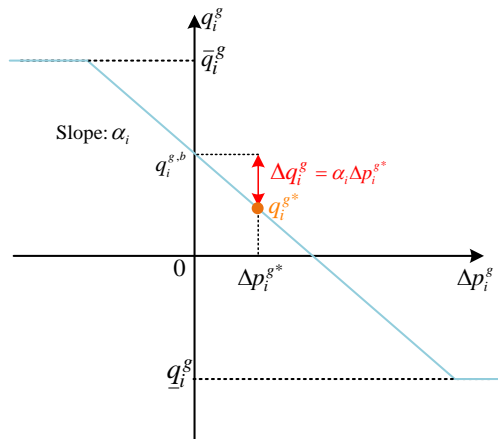


Fig. 1. The reactive power adjustment following an affine 'P-Q' rule

modified IEEE-123 bus system are given in Section V and the paper is concluded in Section VI.

II. TWO-STAGE VVC FRAMEWORK: OVERVIEW

The paper proposes a two-stage VVC framework. Based on the predicted information, the first stage aims to minimize the system power losses by dispatching the optimal settings of switch-based discrete devices and determining the optimal base reactive power set points for PV inverters. Considering the long reaction time of the discrete voltage control devices, the first-stage VVC has a slow timescale. However, only relying on the forecast values, the intermittent nature of PV may cause unexpected voltage deviations. In the second stage, the PV deviation from its forecast value is considered. On the basis of its reactive power set point determined in the first stage, each PV inverter further adjusts its reactive power along with its real-time active power output to avoid potential voltage violations. The reactive power adjustment of PV inverter follows an optimal affine 'P-Q' rule. As shown in Fig.1, $q_i^{g,b}$ is the PV inverter's base reactive power set point determined in the first stage, and Δp_i^{g*} is the PV deviation from its forecast value. Upon the optimal affine 'P-Q' rule, the PV inverters' real-time reactive power can be adjusted as follows:

$$q_i^g = q_i^{g,b} + \Delta q_i^g \quad (1)$$

with

$$\Delta q_i^g = \alpha_i \Delta p_i^{g*} \quad (2)$$

where α_i is the slope of the affine 'P-Q' rule.

The value of α_i is determined by solving an affinely adjustable robust problem with the goal of minimizing voltage deviations caused by the PV fluctuations. Note that voltage sensitivities with respect to active/reactive power injections are the key parameters to determine the optimal affine 'P-Q' rule. Conventionally, the voltage sensitivities can be estimated by inverting the Jacobian matrix or using the perturb and observe method, which could be time-consuming. To this end, we propose a data-driven AARVVC to determine the optimal affine 'P-Q' rule in the second stage. As shown in Fig. 2, the data-driven AARVVC for the second-stage VVC consists of two

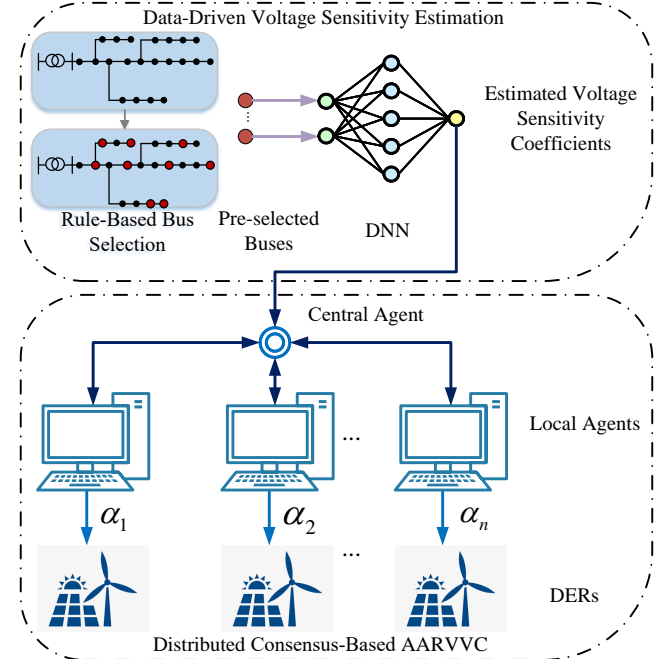


Fig. 2. The data-driven AARVVC for the second-stage VVC

steps: (1) Data-driven voltage sensitivity estimation; (2) Distributed consensus-based AARVVC.

With respect to the data-driven voltage sensitivity estimation, the DNN is utilized to predict voltage sensitivities by using the operating statuses, including the bus active and reactive power injections and voltages, as the input. The operating statuses of each bus can be regarded as one input feature for the DNN. To improve the training efficiency and reduce redundant information behind features, a rule-based bus selection with a BDS process is first utilized to select a subset of buses whose operating statuses have a more important and greater impact on the voltage sensitivity estimation. More details about the rule-based bus selection process are provided in Section IV. Then, the DNN-based voltage sensitivity estimation is performed to predict voltage sensitivities.

Finally, a distributed consensus-based AARVVC is proposed to determine the optimal 'P-Q' rule of each PV inverter in a hierarchical manner after receiving the estimated voltage sensitivities from the DNN. The communication between the local bus agents and the central agent is required for information exchange. As every local bus agent reaches a consensus with the central agent on the optimal 'P-Q' rule, the communication process halts.

III. FIRST-STAGE VVC STRATEGY

The first-stage VVC strategy is a deterministic OPF problem to determine the step positions of discrete devices and the optimal base reactive power set points for PV inverters based on the forecast values of DERs. The objective of this first stage is to minimize the total power losses while maintaining system voltages within the range of [0.95, 1.05].

A. The Distribution Network

Consider a radial distribution network containing $n+1$ buses represented as set $\{0\} \cup \mathcal{N}$, where $\{0\}$ denotes the slack bus at which the distribution network is connected to the transmission network and set $\mathcal{N} := \{1, \dots, n\}$ denotes all other buses. Hence the radial network contains n line segments connecting the adjacent buses. For any bus $j \in \mathcal{N}$, \mathcal{N}_j is the set of all children buses of bus j . The set consisting all line segments in the distribution network can be expressed as: $\mathcal{L} = \{\ell_j = (i, j) | i = b^p(j), j \in \mathcal{N}\}$, where $b^p(j)$ denotes the parent bus of bus j . For each line segment $(i, j) \in \mathcal{L}$, let P_{ij} and Q_{ij} represent the active/reactive power flow through the line respectively, r_{ij} and x_{ij} denote the line resistance and reactance. Let p_i and q_i represent the active and reactive power injections of bus i , V_i and v_i denote the voltage magnitude and the squared voltage magnitude of bus i . Then the linearized distribution power flow [32], [33] can be expressed as:

$$P_{ij} = \sum_{k \in \mathcal{N}_j} P_{jk} - p_j \quad (3a)$$

$$Q_{ij} = \sum_{k \in \mathcal{N}_j} Q_{jk} - q_j \quad (3b)$$

$$v_i - v_j = 2(r_{ij}P_{ij} + x_{ij}Q_{ij}) \quad (3c)$$

B. First-Stage VVC Problem Formulation

On the basis of the linearized distribution power flow, the first-stage VVC problem is formulated as ¹:

$$\min F = \sum_{(i,j) \in \mathcal{L}} r_{ij} \cdot \frac{P_{ij}^2 + Q_{ij}^2}{v_{nom}} \quad (4)$$

subject to:

$$P_{ij} = \sum_{k \in \mathcal{N}_j} P_{jk} + p_j^l - p_j^g, \forall j \in \mathcal{N} \quad (5a)$$

$$Q_{ij} = \sum_{k \in \mathcal{N}_j} Q_{jk} + q_j^l - q_j^g - q_j^c, \forall j \in \mathcal{N} \quad (5b)$$

$$v_i - v_j = 2(r_{ij}P_{ij} + x_{ij}Q_{ij}), \forall (i, j) \in \mathcal{L} \quad (5c)$$

$$v_0 = 1 + 2n_{tap}\Delta tap + (n_{tap}\Delta tap)^2 \approx 1 + 2n_{tap}\Delta tap \quad (5d)$$

$$\underline{n}_{tap} \leq n_{tap} \leq \bar{n}_{tap}, n_{tap} \in \mathbb{Z} \quad (5e)$$

$$|n_{tap} - n_{tap}^p| \leq \Delta n_{tap} \quad (5f)$$

$$q_i^c = n_i^c \cdot \Delta q_i^c, n_i^c \in \mathbb{Z}, \forall i \in \mathcal{N} \quad (5g)$$

$$0 \leq n_i^c \leq \bar{n}_i^c, \forall i \in \mathcal{N} \quad (5h)$$

$$|n_i^c - n_i^{p,c}| \leq \Delta n_i^c, \forall i \in \mathcal{N} \quad (5i)$$

$$-\bar{q}_i^g \leq q_i^g \leq \bar{q}_i^g, \forall i \in \mathcal{N} \quad (5j)$$

$$\bar{q}_i^g = \sqrt{S_i^2 - (p_i^g)^2}, \forall i \in \mathcal{N} \quad (5k)$$

$$v \leq v_i \leq \bar{v}, \forall i \in \mathcal{N} \quad (5l)$$

¹For this first-stage VVC problem, the power losses can be approximated by $\sum_{(i,j) \in \mathcal{L}} r_{ij} \cdot \frac{P_{ij}^2(t) + Q_{ij}^2(t)}{v_{nom}}$ to convexify the optimization problem, like [34], [35].

where (4) represents the first-stage VVC goal is to minimize the total power losses. Constraints (5a)-(5c) are the linearized power flow constraints. Equation (5d) represents the voltage of the swing bus considering the on-load tap changing transformer (OLTC) where n_{tap} denotes the tap position and Δtap denotes the tap step size. A linear approximation is applied to (5d). Equations (5e) and (5f) are the operational constraints of OLTC, where n_{tap}^p is the previous tap position. The operational constraints of capacitor banks and PV inverters are presented in (5g)-(5i) and (5j)-(5k), where $n_i^{p,c}$ denote the previous number of capacitor banks. Equation (5l) is the voltage constraint. Including the settings of the switch-based discrete devices as controllable variables, the first-stage VVC is a mixed-integer optimization problem. By running the first-stage VVC optimization, the optimal step positions of switch-based discrete devices and the base reactive power set points for PV inverters can be obtained. With respect to the first-stage VVC, the optimization variables include:

(1) Exogenous variables:

$$q_i^g, q_i^c, n_i^c, \forall i \in \mathcal{N}, \text{ and } n_{tap}$$

(2) Endogenous variables:

$$P_{ij}, Q_{ij}, \forall (i, j) \in \mathcal{L} \\ v_0, v_i, \forall i \in \mathcal{N}$$

However, the fluctuating nature of PV is not considered in the first-stage VVC, and the real-time PV generation may vary rapidly and deviate from its forecast value, potentially leading to voltage violations. Due to the slow response time of the legacy voltage control devices like OLTCs and capacitor banks, the first-stage VVC may not be capable of dealing with such fast voltage deviations. To this end, a second-stage VVC strategy is proposed to resolve voltage issues by adjusting PV inverters' reactive power in real-time.

IV. SECOND-STAGE VVC STRATEGY: REAL-TIME ADJUSTMENT OF REACTIVE POWER

The second-stage VVC strategy focuses on the real-time adjustment for the reactive power outputs of inverters. In the first stage, the base reactive power set points for inverters are determined based on the forecast values of PV outputs without considering the uncertain characteristic of renewable energy. To avoid potential voltage issues caused by the PV fluctuations, the second-stage VVC is proposed for reactive power adjustment. A 'P-Q' affine rule is applied as the adjustment rule. The reactive power of PV inverter at bus i after the adjustment can be expressed as (6):

$$q_i^{g*} = q_i^{g,b} + \alpha_i \cdot \Delta p_i^g \quad (6)$$

Here the PV inverter reactive power q_i^{g*} can be split into two parts: the non-adjustable (or deterministic) part $q_i^{g,b}$, and the adjustable part which is expressed as an affine function of the PV deviation Δp_i^g with the slope α_i . Note that $q_i^{g,b}$ is the optimization solution of q_i^g in the first-stage VVC. Given the slope α_i , the reactive power adjustment can be calculated immediately with the real-time PV output. Therefore, the second-stage VVC strategy allows the real-time adjustment of PV inverter's

reactive power in accordance with its real-time active power output to mitigate the voltage fluctuation.

A. Second-Stage Problem Formulation: Robust Optimization Solution

The aim of the second-stage VVC strategy is to minimize the system voltage deviations due to the rapid PV fluctuations by adjusting inverters' reactive power following the optimal affine 'P-Q' rule.

Let \mathcal{N}_G denote the set of all buses with PVs installed. For any bus $i \in \mathcal{N}$, its voltage deviation can be estimated based on voltage sensitivity:

$$\Delta V_i = \sum K_{ij}^p \cdot \Delta p_j^q + K_i^q \cdot \Delta q_j^q, \forall j \in \mathcal{N}_G \quad (7)$$

where K_{ij}^p and K_i^q are the voltage sensitivities at bus i to the active and reactive power injections at bus j , respectively.

It is worth mentioning that the PV deviation Δp_j^q from the base PV set point $p_j^{q,b}$ is an uncertain parameter:

$$\Delta p_j^q \in [\Delta p_j^{min}, \Delta p_j^{max}], \forall j \in \mathcal{N}_G \quad (8)$$

where $\Delta p_j^{min} \leq 0$, $\Delta p_j^{max} \geq 0$ indicates that the actual PV outputs can deviate from the predicted values in both positive and negative directions. The second-stage VVC strategy is expected to be robust against the PV output uncertainty.

Considering the uncertain parameter Δp_j^q , the second-stage VVC problem can be formulated as a robust optimization problem:

$$\min \sum_{i=1}^n |\Delta V_i| \quad (9)$$

subject to:

$$(7), (8)$$

To get rid of the absolute value operator in (9), an auxiliary variable V_i^{aux} is introduced, and the problem (9) can be rewritten as follows:

$$\min \sum_{i=1}^n V_i^{aux} \quad (10)$$

subject to:

$$(8)$$

$$V_i^{aux} \geq \sum_{j=1}^n (K_{ij}^p + \alpha_j \cdot K_{ij}^q) \cdot \Delta p_j^q, \forall i \in \mathcal{N}, \forall j \in \mathcal{N}_G \quad (11a)$$

$$V_i^{aux} \geq - \sum_{j=1}^n (K_{ij}^p + \alpha_j \cdot K_{ij}^q) \cdot \Delta p_j^q, \forall i \in \mathcal{N}, \forall j \in \mathcal{N}_G \quad (11b)$$

Given that Δp_j^q varies in the uncertainty interval, the corresponding affinely adjustable robust counterpart (AARC) [36] of (11) can be reformulated as follows:

$$\min \sum_{i=1}^n V_i^{aux} \quad (12)$$

for $\forall i \in \mathcal{N}, \forall j \in \mathcal{N}_G$, subject to:

$$V_i^{aux} \geq \sum_{j=1}^n (\theta'_{ij} \cdot \Delta p_j^{max} + \theta''_{ij} \cdot \Delta p_j^{min}) \quad (13a)$$

$$V_i^{aux} \geq - \sum_{j=1}^n (\theta'_{ij} \cdot \Delta p_j^{min} + \theta''_{ij} \cdot \Delta p_j^{max}) \quad (13b)$$

$$\theta'_{ij} \geq 0 \quad (13c)$$

$$\theta''_{ij} \leq 0 \quad (13d)$$

$$\theta'_{ij} \geq K_{ij}^p + \alpha_j \cdot K_{ij}^q \quad (13e)$$

$$\theta''_{ij} \leq K_{ij}^p + \alpha_j \cdot K_{ij}^q \quad (13f)$$

where θ'_{ij} and θ''_{ij} are the dual variables. Finally, the AARC problem reduces to a linear problem [27], whose solution is the optimal slope α_i for each PV inverter.

With respect to the AARC problem, two main challenges should be considered:

(i) The first one is how to efficiently obtain the values of voltage sensitivities to the active/reactive power injections. Traditional methods to estimate voltage sensitivities, e.g., the inversion of Jacobian matrix and the perturb and observe method, can be time-consuming and complicated.

(ii) What's more is that the AARC problems (12) and (13) are formulated in a centralized manner, which means the central agent needs to collect all the information from local agents, leading to large computational burdens for the central agent.

To this end, we propose a data-driven AARVVC scheme consisting of the data-driven voltage sensitivity estimation and distributed consensus-based AARVVC.

B. Data-Driven Voltage Sensitivity Estimation

Reflecting the impact of power injections change on nodal voltages by projecting the complex power flow relationship into linear space, the voltage sensitivities K_{ij}^p and K_{ij}^q are important parameters in the optimization problem in (12)-(13). In other words, the optimal reactive power adjustment ratio of the affine function in (2) depends on accurate voltage sensitivity calculation. If the accuracy of voltage sensitivity estimation can not be guaranteed, it is difficult to get a reliable affine adjustment ratio, thus significantly affecting the performance of the second-stage VVC. To this end, the data-driven voltage sensitivity estimation method is proposed.

The data-driven voltage sensitivity estimation includes the rule-based bus selection with a BDS process and the DNN-based voltage sensitivity estimation. The rule-based bus selection with a BDS process is applied to select a subset of buses whose operating statuses have a more important and greater impact on the voltage sensitivity estimation, thus improving the training efficiency and reducing redundant information. And the DNN-based voltage sensitivity estimation can efficiently predict voltage sensitivities with high accuracy.

1) Rule-based bus selection with a BDS process: The relationship between the voltage deviations and the deviations of bus power injections is presented as follows:

$$\begin{bmatrix} \Delta p \\ \Delta q \end{bmatrix} = \mathbf{J} \cdot \begin{bmatrix} \Delta \theta \\ \Delta V \end{bmatrix} \quad (14)$$

where \mathbf{J} is the Jacobian matrix, Δp and Δq are the deviations of bus power injections, ΔV and $\Delta \theta$ represent the deviations of voltage magnitudes and angles. This work mainly focuses on the impact of bus power injections on voltage magnitudes. By inverting the Jacobian matrix, the relationship between the

Algorithm 1: BDS-Based Bus Selection

```

S1: Initialization: Define set  $F = \emptyset$  and set  $B = \mathcal{N}$ ,  $m = 0$ , and the number of buses to be selected  $n$ .
S2: SFS process:
Let set  $\mathcal{I} = \{i | i \notin F \text{ and } i \in B\}$ , which contains  $k$  buses  $\{i_1, i_2, \dots, i_k\}$ .
Initialize  $i^* = i_1$ ,  $\eta^* = E(F \cup i_1)$ , where  $E$  is an indicator of estimation error. The larger  $E$  is, the larger the error is.
for  $i = i_1, i_2, \dots, i_k$ ,
     $\eta = E(F \cup i)$ .
    if ( $\eta \leq \eta^*$ )
         $i^* = i$ 
         $\eta^* = \eta$ 
    end if
end for
 $F = F \cup \{i^*\}$ 
S3: SBS process:
Let set  $\mathcal{J} = \{j | j \notin F \text{ and } j \in B\}$  which contains  $l$  buses  $\{j_1, j_2, \dots, j_l\}$ .
Initialize  $j^* = j_1$ ,  $\mu^* = E(B_k - j_1)$ .
for  $j = j_1, j_2, \dots, j_l$ ,
     $\mu = E(B_k - j)$ .
    if ( $\mu \leq \mu^*$ )
         $j^* = j$ 
         $\mu^* = \mu$ 
    end if
end for
 $B = B - \{j^*\}$ 
S4: Let  $m = m+1$ , and go back to S2 until  $m = n$ , which means that the pre-defined number of buses have been selected and added to set  $F$ .

```

deviations of voltage magnitudes and the deviations of bus power injections can be written as:

$$\Delta v = [\ K^p \quad K^q] \cdot \begin{bmatrix} \Delta p \\ \Delta q \end{bmatrix} \quad (15)$$

where K^p and K^q in (15) are sub-matrices of J^{-1} . The operation of matrix inversion can be time-consuming for large-scale systems.

Conventionally, the entries of K^p and K^q can be calculated from the power flow solutions, demanding operating statuses of all buses. However, there is always redundant information behind operating statuses of all buses. By introducing the feature selection process, the information redundancy can be reduced. What's more, from the point of practicality, it is not easy to collect the operating statuses of every single bus and use them for calculating the voltage sensitivities. The rule-based feature selection process can pick out some key buses whose operation statuses contain more valuable information for voltage regulation, which makes the proposed data-driven AARVVC more practical.

To this end, a rule-based bus selection with a BDS Process is utilized to pick the key buses for voltage sensitivity estimation. Only the operating statuses of the selected buses will be used to perform voltage sensitivity estimation.

The operating statuses, including the bus active and reactive power injections and its voltage, of each bus are regarded as one feature, then the bus-selection problem can be converted into a feature-selection problem, which can be resolved by the BDS feature-selection method.

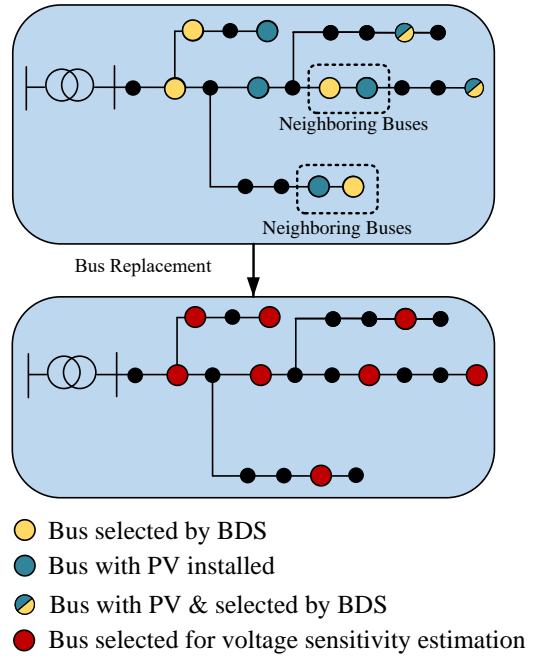


Fig. 3. Merging process of buses selected by BDS and buses with PV installed

As a sequential searching strategy, BDS consists of two separate processes: a sequential forward selection (SFS) which selects the feature that contributes most to improving the estimation accuracy from the remaining feature set, and a sequential backward selection (SBS) that deletes the feature which contributes the least to improving accuracy from the remaining feature set.

The procedure of the BDS is shown in **Algorithm 1: BDS-Based Bus Selection** in detail. In step S2, E represents the estimation error between the true and predicted voltage sensitivities. Every feature from the feature set (B), combines with the set of selected features(F) forming the input for training. As for the feature union with the lowest error, the selected feature from set B is added to set F . In step S3, each feature in the current feature set B is temporarily excluded, and the DNN models are trained based on the remaining feature sets. By comparing the errors, one feature that contributes the least information for voltage sensitivity estimation, which means the well-trained DNN model achieves the highest accuracy without this feature, will be finally removed from the current set B . Note that features selected by SFS will not be deleted by SBS while features removed by SBS will not be selected by SFS. This can ensure that the two processes can converge to the same solution from two directions.

In the second-stage VVC, the PV inverter's reactive power is adjusted in accordance with its real-time active power. It indicates that the operating statuses of buses with PV installed are usually necessary for the AARVVC. From a practical point of view, to reduce the investment in measuring devices, we further define a rule to combine the key buses selected by the BDS process and the buses with PV installed. The rule is defined as follows: if one bus selected by the BDS process is the neighboring bus of any bus with PV installed, then the bus,

selected by the BDS process, will be replaced by its neighboring bus with PV installed. This rule is based on the intuition that there are relatively strong correlations between the operating statuses of two neighboring buses. An illustration example to explain the rule to merge buses selected by BDS and buses with PV installed is depicted in Fig.3.

2) *A DNN-based voltage sensitivity estimation:* The buses, selected by the proposed rule-based bus selection, are used for voltage sensitivity estimation. Instead of requiring the operation statuses of the whole system, only the operating statuses of selected buses are set as the input of DNN. Aiming to establish the mapping relationship from the input features to the voltage sensitivities, supervised machine learning, using a three-layer fully connected DNN, is performed. With the help of the well-trained DNN, the estimated voltage sensitivities can be obtained in real-time. Compared with the conventional methods to calculate the voltage sensitivities, the DNN-based voltage sensitivity estimation can be much more efficient and more capable of coping with the rapidly changing operating statuses of power systems.

C. Distributed Consensus-Based AARVVC

To obtain the slope of the affine ‘P-Q’ rule for PV inverter in a distributed manner, we propose the distributed consensus-based AARVVC to solve the AARC problem (12)-(13). For each bus $i \in \mathcal{N}$, we introduce $\mathbf{z}_i = \{z_i^j | z_i^j = \alpha_j, \forall j \in \mathcal{N}_G\}$, and let $\mathbf{z} = \{\mathbf{z}_i | \forall i \in \mathcal{N}\}$. Then the AARC problem (12)-(13) can be reformulated as follows:

$$\min \sum_{i=1}^n V_i^{aux} \quad (16)$$

for $\forall i \in \mathcal{N}, \forall j \in \mathcal{N}_G$, subject to:

$$V_i^{aux} \geq \sum_{j=1}^n (\theta'_{ij} \cdot \Delta p_j^{\max} + \theta''_{ij} \cdot \Delta p_j^{\min}) \quad (17a)$$

$$V_i^{aux} \geq - \sum_{j=1}^n (\theta'_{ij} \cdot \Delta p_j^{\min} + \theta''_{ij} \cdot \Delta p_j^{\max}) \quad (17b)$$

$$\theta'_{ij} \geq 0 \quad (17c)$$

$$\theta''_{ij} \leq 0 \quad (17d)$$

$$\theta'_{ij} \geq K_{ij}^p + z_i^j * K_{ij}^q \quad (17e)$$

$$\theta''_{ij} \leq K_{ij}^p + z_i^j * K_{ij}^q \quad (17f)$$

$$z_i^j = \alpha_j \quad (17g)$$

Note $\Delta \mathbf{p}^{\min} = [\Delta p_j^{\min}]_{j \in \mathcal{N}_G}, \Delta \mathbf{p}^{\max} = [\Delta p_j^{\max}]_{j \in \mathcal{N}_G}$ are the uncertain parameters, which are assumed to be accessed by each bus $i \in \mathcal{N}$ in this paper, and K_{ij}^p, K_{ij}^q are the voltage sensitivity of bus i with respect to the active and reactive power of bus j , which can be accessed by bus i . It is worth mentioning K_{ij}^p, K_{ij}^q can be estimated by the proposed data-driven voltage sensitivity estimation.

In addition, $\theta'_{ij}, \theta''_{ij}$ can be regarded as the variables associated with bus i . In this case, the objective function (16) as well as the constraints (17a)-(17f) can be split into subproblems related to each bus $i \in \mathcal{N}$. Then, the only coupling constraint is (17g).

Algorithm 2: Distributed Consensus-Based AARVVC

S1: Initialization. Let the number of iterations $k = 1, \alpha(1) = 0, z_i(1) = 0, \lambda_i(1) = 0, \rho > 0$.

S2: Each local bus agent i updates $z_i(k)$ based on the voltage sensitivities K_{ij}^p and K_{ij}^q .

$$z_i(k+1) = \arg \min_{z_i} L_\rho^{(i)}(\alpha(k+1), z_i, \lambda_i(k)) \\ \text{s.t. } (17a) - (17f)$$

S3: Each local agent then communicates $z_i(k+1)$ to the central agent.

S4: Collecting $z_i(k)$ from each local bus agent $i \in \mathcal{N}$, the central agent then updates $\alpha(k+1)$. Each entry $\alpha_j(k+1)$ of $\alpha(k+1)$ can be expressed as:

$$\alpha_j(k+1) = \frac{\sum_{i \in \mathcal{N}} z_i^j(k+1)}{n+1}, \forall i \in \mathcal{N}, \forall j \in \mathcal{N}_G$$

The central agent then sends $\alpha(k+1)$ back to each local bus agent i .

S5: Each local bus agent i updates $\lambda_i(k+1)$:

$$\lambda_i(k+1) = \lambda_i(k) + \rho \cdot (z_i(k+1) - \alpha(k+1)), \forall i \in \mathcal{N}$$

S6: Let $k = k+1$. If $k > k_{max}$, or the consensus is achieved, stop the iteration process; otherwise, go to S2, where k_{max} is the maximum number of iterations.

To deal with the coupling constraint (17g), let $\boldsymbol{\lambda} = \{\lambda_i | i \in \mathcal{N}\}$, where $\lambda_i = \{\lambda_i^j | j \in \mathcal{N}_G\}$, denote dual variables associated with (17g), then the augmented Lagrangian function can be written as:

$$L_\rho(\boldsymbol{\alpha}, \mathbf{z}, \boldsymbol{\lambda}) = \sum_{i=1}^n L_\rho^{(i)}(\alpha_i, \mathbf{z}_i, \lambda_i) \\ = \sum_{i=1}^n \left[V_i^{aux} + \sum_{j \in \mathcal{N}_G} \left(\lambda_i^j \cdot (z_i^j - \alpha_j) + \frac{\rho}{2} \cdot \|z_i^j - \alpha_j\|^2 \right) \right] \quad (18)$$

where ρ is a parameter. Based on ADMM, the problem (16)-(17) can be solved in a distributed manner, which is shown in detail in **Algorithm 2: Distributed Consensus-Based AARVVC**.

As seen in S2 and S3 of Algorithm 2, each local agent is assigned its own subproblem to obtain the optimal values of $z_i(k)$ and then communicates $z_i(k)$ to the central agent using the communication capacity of the inverters during the k -th iteration. Then in step S4, the consensus-based ADMM also simplifies the iteration process and the update of α_j can be realized by simply averaging all entries in the j th column of \mathbf{z} , and the values of α_j are then sent back to corresponding local agents. The local agents then update the dual variable λ_i based on the updated $\boldsymbol{\alpha}$, \mathbf{z}_i and the parameter ρ in step S5. The iteration process will stop until the consensus is achieved among all the local agents or the maximum number of iterations is reached.

V. NUMERICAL RESULTS

In this section, the proposed data-driven AARVVC is implemented on the modified IEEE-123 bus test system to test

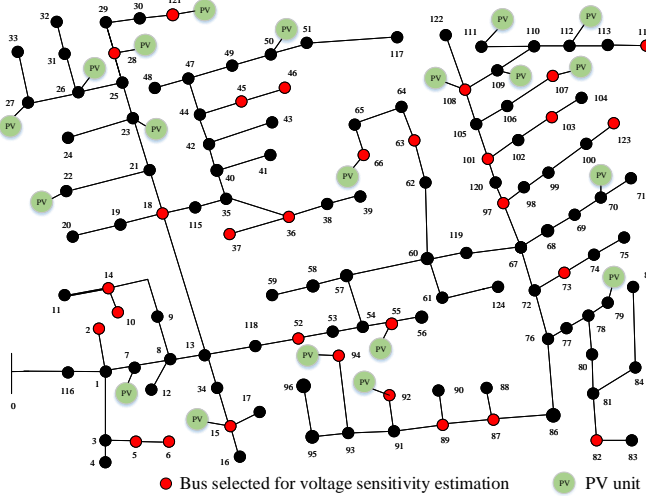


Fig. 4. The modified IEEE-123 bus test system

its performance. The modified IEEE-123 bus test system with PV generators is shown in Fig. 4. The base voltage for the test system is set to 4.16 kV and the base power is set to 100 kVA. The first-stage VVC strategy is run at a circle of 15 minutes based on the forecast PV generations to dispatch the switch-based discrete devices, e.g., OLTC, and determine the base reactive power set points for PV inverters. For the data-driven voltage sensitivity estimation process, 1500 scenarios are generated by randomly setting the nodal power injections, and the real values of voltage sensitivities are obtained by inverting the Jacobian matrices. The dataset is split into three parts of training, validation, and testing, accounting for 80%, 10%, and 10% of data, respectively. The model training, parameter tuning, and testing are conducted offline, then the well-trained model can be utilized for online voltage sensitivity estimation.

In the first-stage VVC, the forecast PV penetration of this system is 47.79%. In the second-stage VVC, a 50% uncertainty interval is considered for each single PV, indicating the uncertainty set of the PV penetration of this system can be 23.89% to 71.68%. Note that the tap positions of discrete devices keep unchanged within the second stage. The reactive power of PV inverter is adjusted following the optimal affine ‘P-Q’ rule, determined by the proposed data-driven AARVVC. In the distributed consensus-based AARVVC, the parameter ρ is set as 0.01 and the maximum number of iterations is set as 100.

A. Voltage Sensitivity Comparisons

As discussed before, the data-driven voltage sensitivity estimation includes two main parts: the bus-selection process and the DNN-based voltage sensitivity estimation, where the operating statuses of these selected buses are used as the input of DNN for voltage sensitivity prediction.

To evaluate the impact of the number of selected buses on the prediction accuracy, the mean average error (MAE) is chosen as the evaluation metric, which can be expressed as fol-

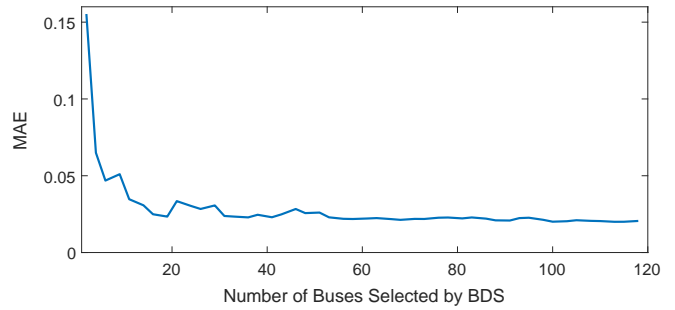


Fig. 5. MAE versus the number of selected buses.

lows:

$$MAE = \frac{1}{n_c} \sum_{i=1}^{n_c} |x_i - \hat{x}_i| \quad (19)$$

where n_c is the number of entries of the predicted voltage sensitivities, x_i represents the real voltage sensitivity and \hat{x}_i is the estimated voltage sensitivity. The number of features to be selected by the bidirectional search process is an important hyperparameter, since it reflects the number of buses whose operation statuses are included in the voltage sensitivity estimation. Setting different numbers of features to be selected by the bidirectional search method and comparing the corresponding MAE on the validation set, Figure 5 shows the relationship of MAE versus the value of buses selected by BDS. As can be seen Fig. 5, MAE first decreases sharply as the number of selected buses increases, then MAE shows slight fluctuations as the number of selected buses is greater than 20. It shows that after the number of selected buses reaches 30, incorporating operating statuses of more buses does not contribute much to improving the prediction accuracy of voltage sensitivity. This phenomenon indicates there is redundant information behind the operating status of all the buses.

In this case, the number of selected buses to perform voltage sensitivity estimation is set to 30. The results of the bus-selection process for the modified IEEE-123 bus test system, selected by the proposed rule-based voltage sensitivity in Section IV, are depicted as red dots in Fig. 4. Those selected buses are distributed across the distribution network. It indicates information coming from almost all parts of the distribution network is incorporated in those selected buses. This might shed light on the reason why using the operating status of part of buses is enough to achieve the accurate voltage sensitivity estimation.

Taking bus 7 as an example, Fig. 6 shows the actual and estimated voltage sensitivities of each bus $i \in \mathcal{N}$ with respect to the active and reactive power injection at bus 7, i.e., dV_i/dp_7 and dV_i/dq_7 for $\forall i \in \mathcal{N}$. The actual voltage sensitivities are calculated by inverting the Jacobian matrix, which are regarded as the benchmark, and the estimated voltage sensitivities are calculated from the proposed data-driven voltage sensitivity estimation method. As shown in Fig. 6, the values of the estimated and actual voltage sensitivities are very close. It validates that the proposed data-driven voltage sensitivity estimation method provides accurate prediction of the

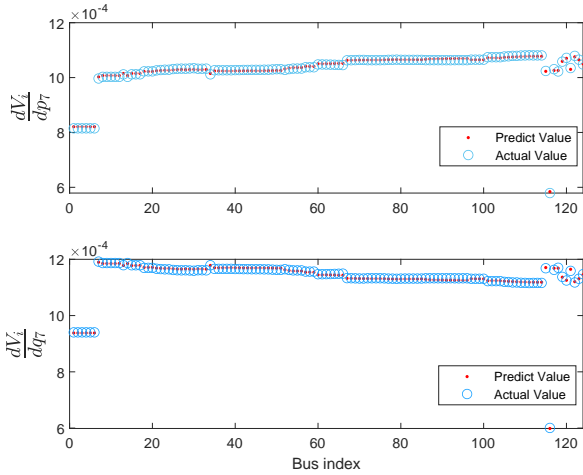


Fig. 6. Actual and estimated voltage sensitivities with respect to active and reactive power injections at bus 7

voltage sensitivities by only making use of the information from the selected buses.

B. Performance of the Distributed Consensus-Based AARVVC

As important parameters, the voltage sensitivities with respect to bus power injections, to decide the slope of the affine ‘P-Q’ rule α_i , it has been validated in subsection V-A that the proposed data-driven voltage sensitivity estimation method can accurately predict voltage sensitivities. We further test the performance of our proposed Algorithm 2: Distributed Consensus-Based AAARVC.

Once the estimated voltage sensitivities are given, the slope α_i of the affine ‘P-Q’ rule for each PV inverter can be determined by our proposed Algorithm 2: Distributed Consensus-Based AAARVC. Taking PV inverters at buses 7, 23, 50 and 107 as an example, the adjustment slopes for those PV inverters, determined by the distributed consensus-based AAARVC, are shown in Fig. 7. The adjustment slopes for those PV inverters solved by the centralized optimization, i.e., the AARC problem (12) and (13) is solved in a centralized manner, are depicted in Fig. 7 as the benchmark. It can be observed from Fig. 7 that all those slopes, determined by the distributed consensus-based AAARVC, can converge to the benchmark, the slopes determined by the centralized optimization. It means that the optimal ‘P-Q’ rules can be accurately calculated by our proposed distributed consensus-based AAARVC in a hierarchical distributed manner.

C. Algorithm Comparisons

For algorithm comparisons, four different VVC schemes are considered:

Scheme 1-First-stage VVC: Only the first-stage VVC is considered.

Scheme 2-Centralized AARVVC with accurate voltage sensitivities: The AARC problem (12) and (13) is solved in a centralized manner, where the voltage sensitivities are obtained by inverting the Jacobian matrix.

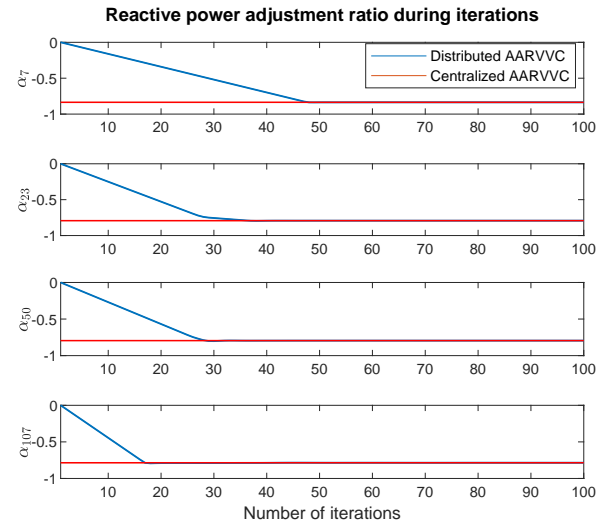


Fig. 7. Slopes for PV inverters at buses 7, 23, 50, and 107

Scheme 3-Distributed consensus-based AARVVC with accurate voltage sensitivities: The AARC problem (12) and (13) is solved in a distributed consensus-based manner, where the voltage sensitivities are obtained by inverting the Jacobian matrix.

Scheme 4-Our proposed data-driven AARVVC, i.e., distributed consensus-based AARVVC with estimated voltage sensitivities: The AARC problem (12) and (13) is solved in a distributed consensus-based manner, where the voltage sensitivities are estimated by the proposed data-driven voltage sensitivity estimation method.

First, consider one extreme scenario, where all the PV generation is at the lowest level within the uncertainty set. The voltage profiles of the modified IEEE-123 bus test system under different schemes are presented in Fig. 8, and the number of buses with voltage violations is given in Table. I. In Fig. 8, the blue curves are the optimal voltage profiles determined in the first stage considering the forecast PV outputs, the yellow curves represent the voltage profiles in different schemes, and the red lines are voltage limits. As shown in Fig. 8, there are voltage violations for a considerable number of buses in Scheme 1. It indicates that without the second-stage reactive power adjustment, the first-stage VVC can not maintain the voltage profiles within the acceptable range. With respect to Scheme 2 and Scheme 3, both of them utilize the accurate voltage sensitivities. The only difference between Scheme 2 and Scheme 3 is the implementation manner, where Scheme 2 is centralized and Scheme 3 is distributed. The outcomes for Scheme 2 and Scheme 3 are virtually identical, it validates our proposed distributed consensus-based AAARVC can converge to the optimal solution solved by the centralized optimization, but it is more scalable and practical. As shown in Table. I, there is only one bus with voltage violations for Scheme 1 and 2, where the lowest bus voltage magnitude for Scheme 2 and Scheme 3 is 0.949 p.u., which is very close to 0.95. For Scheme 4, its outcomes are very close to Scheme 2 and Scheme 3. The only minor difference is the number of buses

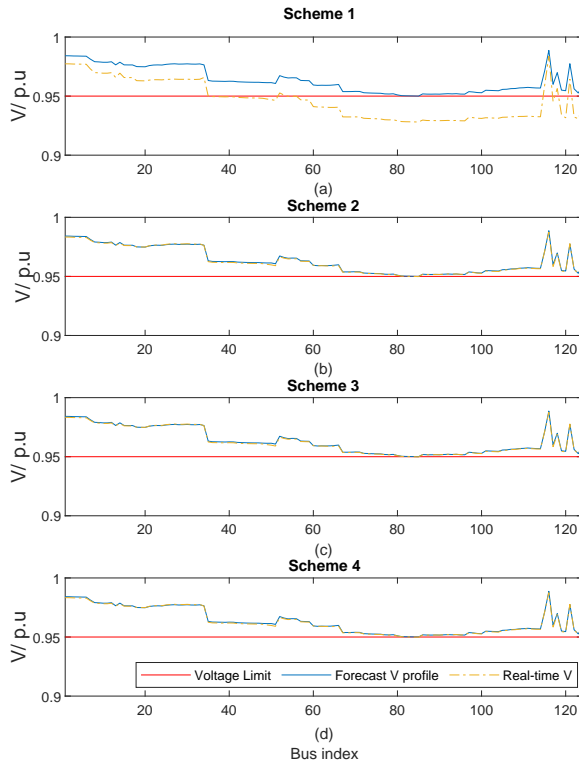


Fig. 8. The voltage profiles of different schemes under an extreme scenario

with voltage violations is 2 for Scheme 4, slightly larger than Schemes 2 and 3. Such a minor difference might be caused by the error between the accurate and estimated voltage sensitivities. The extreme scenario shows that the proposed data-driven AARVVC can achieve a great performance in terms of voltage regulation. To further explore the performance of our proposed

TABLE I
NUMBER OF BUSES WITH VOLTAGE VIOLATIONS UNDER ONE EXTREME SCENARIO

Scheme	1	2	3	4
Bus with Voltage Violations	75	1	1	2
Lowest Voltage (p.u.)	0.929	0.949	0.949	0.949

data-driven AARVVC for voltage regulation, a Monte-Carlo simulation is carried out to randomly generate 1500 scenarios, where the PV active power output is uniformly sampled from its respective uncertainty interval. The distributions of bus voltage magnitudes under different control schemes are presented in Fig. 9. As can be seen in Fig. 9, under Scheme 1, voltages can not be maintained within the pre-defined range and the lowest voltage can be lower than 0.94. For the other 3 schemes, voltages can always be maintained within the acceptable level in most scenarios. Table. II provides the ratios of bus voltage violation under different schemes. Without the second-stage VVC, 7.73 % buses are operated under voltage violations while the proposed data-driven AARVVC method can greatly decrease the ratio to around 0.5%, which is very close to the optimal performance of Scheme 2 and Scheme 3.

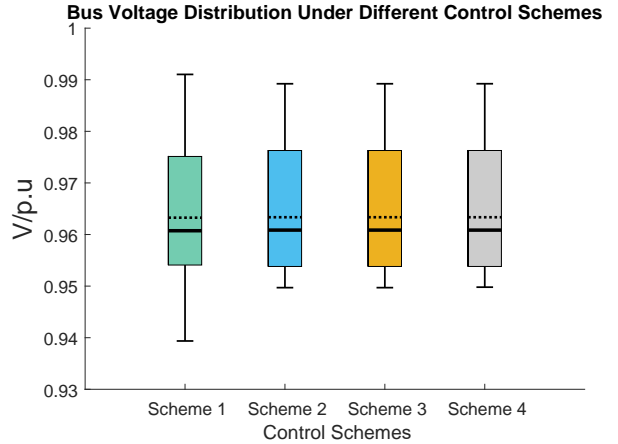


Fig. 9. Distribution of system bus voltage under different control schemes

The lowest voltage for Scheme 4 is slightly lower than 0.95 p.u.. Note that Scheme 3 is also based on our proposed distributed consensus-based AARVVC. Scheme 3 and Scheme 4 are more scalable and require fewer computation burdens compared to Scheme 2. Even though the performance of Scheme 4 is slightly inferior to Scheme 3, it is more computationally efficient as it intelligently relies on the DNN to predict voltage sensitivities.

As summarized in Table. III, the proposed AARVVC can greatly improve the voltage issues in the system, but requires only operation information from partial buses and no topology information. With the hierarchical distributed solution structure, it has better scalability and information privacy.

TABLE II
PERCENTAGE OF BUSES WITH VOLTAGE VIOLATIONS UNDER 1500 SCENARIOS

Scheme	1	2	3	4
Percentage of Buses with voltage violation (%)	7.73	0.47	0.47	0.53
Lowest Voltage (p.u.)	0.939	0.949	0.949	0.949

D. Comparisons with Other Techniques

To further demonstrate the performance of our proposed AARVVC method, comparisons with two other voltage regulation strategies are conducted.

The first one is the constant power factor (CPF) strategy. As suggested in [2], DERs' power factor settings can be specified by the system operator. Then local DERs can adjust the reactive power following the power factor without exceeding the inverters' capability. In the first stage VVC, the optimal set points of PV inverters' reactive power q^g can be obtained. Based on p^g and q^g , the power factor can be calculated. Then the second stage adjustment aims to maintain the constant power factor as:

$$\frac{q^g}{p^g} = \frac{q^g + \Delta q^{PF}}{p^g + \Delta p^g} \quad (20a)$$

TABLE III
SUMMARY OF THE 4 SCHEMES

Scheme	Second stage adjustment	Voltage issues	Topology information required	Operation statuses required	Scalability and Privacy Issues
1	w/o	Serious	/	/	/
2	w	Greatly improved	Yes	All buses	Yes
3	w	Greatly improved	Yes	All buses	No
4	w	Greatly improved	No	Partial buses	No

$$\Delta q^{PF} = \frac{q^g}{p^g} \cdot \Delta p \quad (20b)$$

Another technique is the fixed droop control (FDC) suggested by [2] with a dead band. Under this control strategy, the PV inverter should control its reactive power output following a piecewise linear relationship with voltage.

TABLE IV
COMPARISONS WITH OTHER TECHNIQUES

Strategy	Percentage of Buses with voltage violation (%)	Lowest voltage (p.u.)
AARVVC	0.53	0.949
CPF	13.61	0.930
FDC	3.64	0.943

By conducting a Monte-Carlo simulation with 1500 randomly generated scenarios, the performance of different voltage regulation strategies is summarized in Table. IV. Among all three strategies, our AARVVC achieves the best performance, with only 0.53% nodes experiencing voltage violations. The CPF strategy performs worst. As a result, the voltage support from the PV inverters gets further weakened. With the default settings of parameters, the FDC can effectively reduce voltage violations, but the performance is not as good as the proposed AARVVC.

E. Extension to Load Uncertainty

It is worth mentioning that our proposed AARVVC can be easily extended to consider load uncertainties by making some minor modifications. See Appendix A for more details about it.

In this subsection, to make our proposed AARVVC more generally applicable to various scenarios, the uncertainty of nodal active and reactive power loads is considered. For the second stage VVC, in addition to the PV uncertainty, a 10% percent uncertainty interval of both active and reactive power loads is considered for each bus.

A Monte-Carlo simulation with 1500 randomly generated scenarios is carried out to test the performance of the extended AARVVC under the uncertainty of both loads and PV generation. The PV active power outputs, as well as active and reactive power loads are uniformly sampled from their uncertain interval. For comparison, a base case without any second-stage adjustment is conducted.

TABLE V
PERCENTAGE OF BUSES WITH VOLTAGE VIOLATIONS

Second stage adjustment	Percentage of Buses with voltage violation (%)	Lowest voltage (p.u.)
w/o	20.74	0.927
w	1.59	0.948

As can be seen in Table. V, our proposed AARVVC can also effectively mitigate voltage issues with considerations of both load and PV uncertainties. For the base case, the percentage of bus voltage violations increases greatly to 20.74%, meanwhile the lowest bus voltage can be as low as 0.927 p.u.. In contrast, after the extended form of the AARVVC is carried out, the occurrence of voltage violations is drastically reduced to 1.59% and the lowest bus voltage can be maintained at 0.948. The results validate the capability of the extended AARVVC to deal with the load uncertainty.

VI. CONCLUSION

This paper introduces a data-driven AARVVC strategy for voltage regulation against PV and load uncertainties. The data-driven AARVVC strategy includes two parts: the data-driven voltage sensitivity estimation and the distributed consensus-based AARVVC, which are performed in a distributed manner with the estimated voltage sensitivities. The voltage sensitivities are efficiently predicted by the DNN with the operating statuses of selected buses as the input. The effectiveness and superiority of the proposed data-driven AARVVC strategy are tested on the modified IEEE-123 bus test system. The results show it can accurately and efficiently estimate voltage sensitivities and achieve a good voltage regulation performance in a distributed consensus-based manner. In the future, we will take into account the network topology change.

ACKNOWLEDGEMENT

This article has been authored by an employee of National Technology & Engineering Solutions of Sandia, LLC under Contract No. DE-NA0003525 with the U.S. Department of Energy (DOE). The employee owns all right, title and interest in and to the article and is solely responsible for its contents. The United States Government retains and the publisher, by accepting the article for publication, acknowledges that the United States Government retains a non-exclusive, paid-up,

irrevocable, world-wide license to publish or reproduce the published form of this article or allow others to do so, for United States Government purposes. The DOE will provide public access to these results of federally sponsored research in accordance with the DOE Public Access Plan: <https://www.energy.gov/downloads/doe-public-access-plan>.

APPENDIX A

Extension to load uncertainties:

The proposed AARVVC method can be further extended to take the load uncertainty into consideration. Let Δp^l and Δq^l denote the active and reactive power load uncertainty, respectively. The voltage deviations in (7) can be further expressed as follows:

$$\begin{aligned}\Delta V_i &= \sum_{j=1}^n K_{ij}^p \cdot (\Delta p_j^g - \Delta p_j^l) + K_{ij}^q \cdot (\Delta q_j^g - \Delta q_j^l), \\ &= \sum_{j=1}^n K_{ij}^p \cdot (\Delta p_j^g - \Delta p_j^l - \frac{K_{ij}^q}{K_{ij}^p} * \Delta q_j^l) + K_{ij}^q \cdot \Delta q_j^g \\ &= \sum_{j=1}^n K_{ij}^p \cdot \Delta p_j^{i*} + K_{ij}^q \cdot \Delta q_j^g, \forall i, j \in \mathcal{N}\end{aligned}\quad (21)$$

Let $\Delta p_j^{i*} = \Delta p_j^g - \Delta p_j^l - \frac{K_{ij}^q}{K_{ij}^p} * \Delta q_j^l$, then equation (21) can be written as:

$$\Delta V_i = \sum_{j=1}^n K_{ij}^p \cdot \Delta p_j^{i*} + K_{ij}^q \cdot \Delta q_j^g, \forall i, j \in \mathcal{N} \quad (22)$$

Note that ΔV_i considers the influences from both PV and load uncertainties here, instead of only PV uncertainties. The formulation in (12) and (13) can be reformulated as:

$$\min \sum_{i=1}^n V_i^{aux} \quad (23)$$

subject to:

$$\Delta p_j^{i*} \in [\underline{\Delta p_j^{i*}}, \overline{\Delta p_j^{i*}}], \forall j \in \mathcal{N} \quad (24a)$$

$$V_i^{aux} \geq \sum_{j=1}^n (K_{ij}^p + \alpha_j \cdot K_{ij}^q) \cdot \Delta p_j^{i*}, \forall i, j \in \mathcal{N} \quad (24b)$$

$$V_i^{aux} \geq - \sum_{j=1}^n (K_{ij}^p + \alpha_j \cdot K_{ij}^q) \cdot \Delta p_j^{i*}, \forall i, j \in \mathcal{N} \quad (24c)$$

Then the corresponding affinely adjustable robust counterpart can be written as:

$$\min \sum_{i=1}^n V_i^{aux} \quad (25)$$

for $\forall i, j \in \mathcal{N}$, subject to:

$$V_i^{aux} \geq \sum_{j=1}^n \left(\theta'_{ij} \cdot \underline{\Delta p_j^{i*}} + \theta''_{ij} \cdot \overline{\Delta p_j^{i*}} \right) \quad (26a)$$

$$V_i^{aux} \geq - \sum_{j=1}^n \left(\theta'_{ij} \cdot \underline{\Delta p_j^{i*}} + \theta''_{ij} \cdot \overline{\Delta p_j^{i*}} \right) \quad (26b)$$

$$\theta'_{ij} \geq 0 \quad (26c)$$

$$\theta''_{ij} \leq 0 \quad (26d)$$

$$\theta'_{ij} \geq K_{ij}^p + \alpha_j \cdot K_{ij}^q \quad (26e)$$

$$\theta''_{ij} \leq K_{ij}^p + \alpha_j \cdot K_{ij}^q \quad (26f)$$

Similarly, this problem can be solved by our proposed AARVVC strategy to determine the 'P-Q' rule.

REFERENCES

- [1] *American National Standard for Electric Power Systems and Equipment Voltage Ratings (60 Hz)*, American National Standards Institute (ANSI) C84.1, 2016.
- [2] *IEEE Standard for Interconnection and Interoperability of Distributed Energy Resources with Associated Electric Power Systems Interfaces*, IEEE Std 1547-2018, 2018.
- [3] M. Farivar, R. Neal, C. Clarke, and S. Low, "Optimal inverter VAR control in distribution systems with high PV penetration," in *Proc. IEEE Power Energy Soc. General Meeting*, 2012, pp.1-7.
- [4] H. Sun, Q. Guo, J. Qi, V. Ajjarapu, R. Bravo, J. Chow, Z. Li, R. Moghe, E. Nasr-Azadani, U. Tamrakar, G. N. Taranto, R. Tonkoski, G. Valverde, Q. Wu, and G. Yang, "Review of challenges and research opportunities for voltage control in smart grids," *IEEE Trans. Power Syst*, vol. 34, no. 4, pp. 2790–2801, Jul, 2019.
- [5] T. Ding, S. Liu, W. Yuan, Z. Bie, and B. Zeng, "A two-stage robust reactive power optimization considering uncertain wind power integration in active distribution networks," *IEEE Trans. Sustain. Energy*, vol. 7, no. 1, pp. 301–311, Jan. 2016.
- [6] G. Qu and N. Li, "Optimal distributed feedback voltage control under limited reactive power," *IEEE Trans. Power Syst.*, vol. 35, no. 1, pp. 315–331, Jan. 2020.
- [7] N. Yorino, Y. Zoka, M. Watanabe, and T. Kurushima, "An optimal autonomous decentralized control method for voltage control devices by using a multi-agent system," *IEEE Trans. Power Syst.*, vol. 30, no. 5, pp. 2225–2233, Sep. 2015.
- [8] H. Ahmadi, J. R. Martí, and H. W. Dommel, "A framework for volt-var optimization in distribution systems," *IEEE Trans. Smart Grid*, vol. 6, no. 3, pp. 1473–1483, May. 2015.
- [9] T. Ding, S. Liu, W. Yuan, Z. Bie, and B. Zeng, "A two-stage robust reactive power optimization considering uncertain wind power integration in active distribution networks," *IEEE Trans. Sustain. Energy*, vol. 7, no. 1, pp. 301–311, Jan. 2016.
- [10] D. K. Molzahn, F. Dörfler, H. Sandberg, S. H. Low, S. Chakrabarti, R. Baldick, and J. Lavaei, "A survey of distributed optimization and control algorithms for electric power systems," *IEEE Trans. Smart Grid*, vol. 8, no. 6, pp. 2941–2962, Nov. 2017.
- [11] S. Boyd, N. Parikh, E. Chu, B. Peleato, J. Eckstein, et al., "Distributed optimization and statistical learning via the alternating direction method of multipliers," *Foundations and Trends® in Machine learning*, vol. 3, no. 1, pp. 1–122, 2011.
- [12] P. Li, C. Zhang, Z. Wu, Y. Xu, M. Hu, and Z. Dong, "Distributed adaptive robust voltage/var control with network partition in active distribution networks," *IEEE Trans. Smart Grid*, vol. 11, no. 3, pp. 2245–2256, May. 2020.
- [13] R. Cheng, Z. Wang, Y. Guo, and Q. Zhang, "Online voltage control for unbalanced distribution networks using projected newton method," *IEEE Trans. Power Syst.*, pp. 1–1, in press, 2022.
- [14] Y. Guo, H. Gao, H. Xing, Q. Wu, and Z. Lin, "Decentralized coordinated voltage control for VSC-HVDC connected wind farms based on ADMM," *IEEE Trans. Sustain. Energy*, vol. 10, no. 2, pp. 800–810, Apr. 2019.
- [15] Y. Wang, T. Zhao, C. Ju, Y. Xu, and P. Wang, "Two-level distributed volt/var control using aggregated PV inverters in distribution networks," *IEEE Trans. Power Del.*, vol. 35, no. 4, pp. 1844–1855, Aug. 2020.
- [16] C. Zhang, Y. Xu, Y. Wang, Z. Y. Dong, and R. Zhang, "Three-stage hierarchically-coordinated voltage/var control based on pv inverters considering distribution network voltage stability," *IEEE Trans. Sustain. Energy*, vol. 13, no. 2, pp. 868–881, Apr. 2022.
- [17] S. Maharjan, A. M. Khambadkone, and J. C.-H. Peng, "Robust constrained model predictive voltage control in active distribution networks," *IEEE Trans. Sustain. Energy*, vol. 12, no. 1, pp. 400–411, Jan. 2021.
- [18] P. Jahangiri and D. C. Aliprantis, "Distributed volt/var control by PV inverters," *IEEE Trans. Power Syst*, vol. 28, no. 3, pp. 3429–3439, 2013.

- [19] H. Zhu and H. J. Liu, "Fast local voltage control under limited reactive power: Optimality and stability analysis," *IEEE Trans. Power Syst.*, vol. 31, no. 5, pp. 3794–3803, 2016.
- [20] M. Farivar, L. Chen, and S. Low, "Equilibrium and dynamics of local voltage control in distribution systems," in *52nd IEEE Conference on Decision and Control*, pp. 4329–4334, 2013.
- [21] N. Li, G. Qu, and M. Dahleh, "Real-time decentralized voltage control in distribution networks," in *2014 52nd Annual Allerton Conference on Communication, Control, and Computing (Allerton)*, pp. 582–588, 2014.
- [22] A. Singhal, V. Ajjarapu, J. Fuller, and J. Hansen, "Real-time local volt/var control under external disturbances with high PV penetration," *IEEE Trans. Smart Grid*, vol. 10, no. 4, pp. 3849–3859, 2019.
- [23] R. Cheng, N. Shi, S. Maharjan, and W. Zhaoyu, "Automatic self-adaptive local voltage control under limited reactive power," *IEEE Trans. Smart Grid*, to appear, 2023.
- [24] F. U. Nazir, B. C. Pal, and R. A. Jabr, "Distributed solution of stochastic volt/var control in radial networks," *IEEE Trans. Smart Grid*, vol. 11, no. 6, pp. 5314–5324, Nov. 2020.
- [25] A. Reza Malekpour and A. Pahwa, "A dynamic operational scheme for residential PV smart inverters," *IEEE Trans. Smart Grid*, vol. 8, no. 5, pp. 2258–2267, Sep. 2017.
- [26] F. Tamp and P. Ciufo, "A sensitivity analysis toolkit for the simplification of MV distribution network voltage management," *IEEE Trans. Smart Grid*, vol. 5, no. 2, pp. 559–568, Mar. 2014.
- [27] R. A. Jabr, "Robust volt/var control with photovoltaics," *IEEE Trans. Power Syst.*, vol. 34, no. 3, pp. 2401–2408, May. 2019.
- [28] S. M. N. R. Abadi, A. Attarha, P. Scott, and S. Thiébaux, "Affinely adjustable robust volt/var control for distribution systems with high PV penetration," *IEEE Trans. Power Syst.*, vol. 36, no. 4, pp. 3238–3247, Jul. 2021.
- [29] F. Ul Nazir, B. C. Pal, and R. A. Jabr, "Affinely adjustable robust volt/var control without centralized computations," *IEEE Trans. Power Syst.*, pp. 1–1, Mar. 2022.
- [30] Z. Zhang, L. F. Ochoa, and G. Valverde, "A novel voltage sensitivity approach for the decentralized control of DG plants," *IEEE Trans. Power Syst.*, vol. 33, no. 2, pp. 1566–1576, Mar. 2018.
- [31] H. Liu and H. Motoda, *Feature selection for knowledge discovery and data mining*, vol. 454. Springer Science & Business Media, 2012.
- [32] M. E. Baran and F. F. Wu, "Optimal capacitor placement on radial distribution systems," *IEEE Trans. Power Del.*, vol. 4, no. 1, pp. 725–734, Jan. 1989.
- [33] M. E. Baran and F. F. Wu, "Network reconfiguration in distribution systems for loss reduction and load balancing," *IEEE Power Engineering Review*, vol. 9, no. 4, pp. 101–102, 1989.
- [34] C. Zhang and Y. Xu, "Hierarchically-coordinated voltage/var control of distribution networks using PV inverters," *IEEE Trans. Smart Grid*, vol. 11, no. 4, pp. 2942–2953, 2020.
- [35] Y. Xu, Z. Y. Dong, R. Zhang, and D. J. Hill, "Multi-timescale coordinated voltage/var control of high renewable-penetrated distribution systems," *IEEE Trans. Power Syst.*, vol. 32, no. 6, pp. 4398–4408, 2017.
- [36] A. Ben-Tal, A. Goryashko, E. Guslitzer, and A. Nemirovski, "Adjustable robust solutions of uncertain linear programs," *Mathematical programming*, vol. 99, no. 2, pp. 351–376, 2004.



Rui Cheng (Graduate Student Member, IEEE) is currently a Ph.D. student in the Department of Electrical & Computer Engineering at Iowa State University. He received the B.S. degree in electrical engineering from Hangzhou Dianzi University in 2015 and the M.S. degree in electrical engineering from North China Electric Power University in 2018. His research interests include power distribution systems, voltage/var control, transactive energy markets, and applications of optimization and machine learning methods to power systems.



Liming Liu (Graduate Student Member, IEEE) is presently pursuing his Ph.D. in the Department of Electrical & Computer Engineering at Iowa State University. He received his B.S. degree and M.S. degree in Electrical Engineering from North China Electric Power University in 2016 and 2019, respectively. His research interests encompass power distribution systems, distribution system modeling, and the application of optimization and machine learning techniques to power systems.



Zhaoyu Wang (Senior Member, IEEE) received the B.S. and M.S. degrees in electrical engineering from Shanghai Jiao Tong University, and the M.S. and Ph.D. degrees in electrical and computer engineering from Georgia Institute of Technology. He is the Northrop Grumman Endowed Associate Professor with Iowa State University. His research interests include optimization and data analytics in power distribution systems and microgrids. He was the recipient of the National Science Foundation CAREER Award, the Society-Level Outstanding Young Engineer Award from IEEE Power and Energy Society (PES), the Northrop Grumman Endowment, College of Engineering's Early Achievement in Research Award, and the Harpole-Pentair Young Faculty Award Endowment. He is the Principal Investigator for a multitude of projects funded by the National Science Foundation, the Department of Energy, National Laboratories, PSERC, and Iowa Economic Development Authority. He is the Co-TCPC of IEEE PES PSOPE, the Chair of IEEE PES PSOPE Award Subcommittee, the Vice Chair of PES Distribution System Operation and Planning Subcommittee, and the Vice Chair of PES Task Force on Advances in Natural Disaster Mitigation Methods. He is an Associate Editor of IEEE TRANSACTIONS ON SUSTAINABLE ENERGY, IEEE OPEN ACCESS JOURNAL OF POWER AND ENERGY, IEEE POWER ENGINEERING LETTERS, and IET Smart Grid. He was an Associate Editor for IEEE TRANSACTIONS ON POWER SYSTEMS and IEEE TRANSACTIONS ON SMART GRID.



Naihao Shi (Graduate Student Member, IEEE) received the B.S. degree in electrical engineering from North China Electric Power University in 2017 and the M.S. degree in electrical engineering from the George Washington University in 2020. He is currently a Ph.D. student in the Department of Electrical and Computer Engineering, Iowa State University, Ames, IA, USA. His research interests include distribution system modeling, voltage/var control, and applications of optimization in power systems.



Qianzhi Zhang (Member, IEEE) received the Ph.D. degree in Electrical Engineering from Iowa State University, Ames, IA, USA, in 2022. He is currently an Ezra SYSEN postdoc researcher in the System Engineering at Cornell University, Ithaca, USA. He was a recipient of the Outstanding Reviewer Award from IEEE Transaction on Smart Grid and IEEE Transaction on Power Systems. His research interests include power/energy management, voltage/var control, system resilience enhancement, transportation electrification, and the applications of advanced optimization and machine learning techniques in power and energy systems.



MATTHEW J. RENO (SM'09) is a Principal Member of Technical Staff in the Electric Power Systems Research Department at Sandia National Laboratories. His research focuses on distribution system modelling and analysis with high penetration PV, including advanced software tools for automated analysis of hosting capacity, PV interconnection studies, and rapid Quasi-Static Time Series simulations. Matthew is also involved with the IEEE Power System Relaying Committee for developing guides and standards for protection of microgrids and systems with high penetrations of inverter-based resources. He received his Ph.D. in electrical engineering from Georgia Institute of Technology and has been at Sandia for the last 15 years.